

FULL PAPER

Open Access



Small-displacement linear surface ruptures of the 2016 Kumamoto earthquake sequence detected by ALOS-2 SAR interferometry

Satoshi Fujiwara*, Hiroshi Yarai, Tomokazu Kobayashi, Yu Morishita, Takayuki Nakano, Basara Miyahara, Hiroyuki Nakai, Yuji Miura, Haruka Ueshiba, Yasuaki Kakiage and Hiroshi Une

Abstract

We constructed and analyzed the ground surface displacement associated with the 2016 Kumamoto earthquake sequence using satellite radar interferometry images of the Advanced Land Observing Satellite 2. The radar interferogram generally shows elastic deformation caused by the main earthquakes, but many other linear discontinuities showing displacement are also found. Approximately 230 lineaments are identified, some of which coincide with the positions of known active faults, such as the main earthquake faults belonging to the Futagawa and Hinagu fault zones and other minor faults; however, there are much fewer known active faults than lineaments. In each area, the lineaments have a similar direction and displacement to each other; therefore, they can be divided into several groups based on location and major features. Since the direction of the lineaments coincides with that of known active faults or their conjugate faults, the cause of the lineaments must be related to the tectonic stress field of this region. The lineaments are classified into the following two categories: (1) main earthquake faults and their branched subfaults and (2) secondary faults that are not directly related to the main earthquake but whose slip was probably triggered by the main earthquake or aftershocks.

Keywords: 2016 Kumamoto earthquake sequence, ALOS-2, SAR interferometry, Linear surface rupture

Introduction

The 2016 Kumamoto earthquake sequence in Japan caused large crustal deformation, and exposed faults have been identified by ground surveys (Geological Survey of Japan 2016; Goto et al. 2016; Kumahara et al. 2016; Shirahama et al. 2016) and aerial photographs (Nakano et al. 2016). It is difficult to achieve a comprehensive and efficient survey using ground surveys and/or aerial photographs, however, because both methods are unable to detect small displacements of several centimeters, and the ability to make repeated surveys is limited.

In this study, we use radar interferometry from space. In May 2014, the Japan Aerospace Exploration Agency

(JAXA) launched an L-band synthetic aperture radar (SAR) satellite, known as the Advanced Land Observing Satellite 2 (ALOS-2). ALOS-2 has three main advantages for observation of this earthquake sequence. The first is the wavelength of emitted microwaves. In general, L-band SAR interferometry (InSAR) is advantageous for detecting ground displacements, even in vegetated areas, due to its high coherence, compared with C- or X-band microwaves (Kobayashi et al. 2011). This capability enables us to capture the entire crustal deformation, even in vegetated mountainous areas. The second advantage is a right-and-left looking observation capability. Using this right-and-left looking observation from both ascending and descending orbits, surface deformation analysis is available not only in 2.5-D (Fujiwara et al. 2000a) but also in full 3-D (Morishita et al. 2016). The third advantage is repeat observations over a short time period. In

*Correspondence: fujiwara-s2vq@mlit.go.jp
Geospatial Information Authority of Japan, 1 Kitasato, Tsukuba, Ibaraki 305-0811, Japan

the Kumamoto earthquake sequence, the first large earthquake with a moment magnitude (M_w) of 6.2 [Japan Meteorological Agency (JMA) 2016a] occurred on April 14 (JST), and the main and largest earthquake (M_w 7.0) occurred on April 16. Furthermore, many aftershocks and related earthquakes occurred over a relatively long duration and wide area (JMA 2016b), and repeat observations in a short period by ALOS-2 effectively monitored the earthquake sequence. Consequently, InSAR using ALOS-2 is an effective tool for estimating the tectonic stress field of the earthquake sequence.

Generally speaking, interferograms of a large earthquake show elastic deformation caused by the main earthquake fault movement. However, Fujiwara et al. (2000a, b), Fukushima et al. (2013), Guerrieri et al. (2010), Nishimura et al. (2008) and Wei et al. (2011) reported that lineaments representing small displacements appear on interferograms, and Oskin et al. (2012) reported that small displacements appear in differential LiDAR images.

In this study, we detect the displacement field on the ground surface associated with the 2016 Kumamoto earthquake sequence using ALOS-2 InSAR and map a large amount of linear surface ruptures with small displacements. Using InSAR, we can map linear surface ruptures throughout the image with minimal error and analyze the direction and amount of each displacement.

Methods

The Geospatial Information Authority of Japan (GSI) is able to detect detailed co-seismic and post-seismic ground surface deformation through analyses of ALOS-2 interferograms (GSI 2016) for the purpose of disaster response and mitigation. ALOS-2 data were processed using GSISAR software (Fujiwara and Tobita 1999; Fujiwara et al. 1999; Tobita et al. 1999; Tobita 2003). The interferograms used in this study are listed in Table 1, and typical interferograms are shown in Fig. 1a, b. The other interferograms are shown in Additional file 1: Figure A.

We mapped the lineaments in interferograms taken from different satellite positions. Some of the largest noise in an interferogram is atmospheric noise; however, since atmospheric noise has a longer wavelength (Fujiwara et al. 1998), the short wavelength lineaments in the interferograms were probably not associated with atmospheric noise. Moreover, the lineaments were found in several interferograms taken on different dates, and it is unlikely that the same atmospheric effects occurred on different data acquisition dates. A 10-m mesh DEM (GSI 2014) was used to remove the effect of topography; therefore, errors in the DEM would propagate into the deformation results, depending on the baseline characteristics (Hanssen 2001). However, because the displacements of

each lineament are not related to their baseline and these lineaments were not found in the interferograms taken before and after the Kumamoto earthquake sequence, as well as the fact that accuracy of the DEM was 5 m (GSI 2014), the DEM error was small enough to not affect the lineaments. Therefore, the clear, long lineaments identified in this study were likely caused by seismic activity (Fig. 2).

We called the lineaments “linear surface ruptures” in this study. The linear surface ruptures were derived from linear phase discontinuities and/or offsets showing displacement in the interferograms. It should be noted that linear surface ruptures do not equal earthquake faults because, in this study, they were derived from the form of displacement. Since one of the purposes of this study is to find hidden faults, we attempted to remove displacements that did not show horizontal linearity such as landslides. Landslides were fairly easy to identify because they tend to occur as rounded mass movements on a hillside or hilltop that then move downslope.

Fujiwara et al. (2000a, b) and Price and Sandwell (1998) used surface displacement gradient maps to visualize lineaments; however, gradient maps were not necessary in this study because the ALOS-2 interferograms were of very high quality compared with those from other satellites, and acquisition of several images from different satellite positions enabled us to easily identify the lineaments. In this study, we used coherence maps of the interferograms as a supplementary tool for identifying linear surface ruptures. Figure 3 shows an example of the coherence map and identified linear surface ruptures. In general, low coherence of the interferogram occurs when scatter of the InSAR image pixels moves randomly (pixel spacing is several meters or more). Narrow belts of low coherency were found along the linear surface ruptures for two reasons. One is the phase discontinuity of the interferogram, and the other is steep deformation along the linear surface rupture, which are likely to change the shape and structure of the ground surface and cause low coherence of the interferogram by interferometric phase variation due to deformation gradients (Hanssen 2001).

Results

General features of linear surface ruptures

We found approximately 230 linear surface ruptures, for example in the somma (outer rim of the caldera) of Aso volcano, along the Futagawa and Hinagu fault zones, and even in Kumamoto city center. The following are general features of the linear surface ruptures.

1. No linear surface ruptures are apparent in the interferograms taken before 1 pm on April 15 (JST) (in

Table 1 List of ALOS-2 images analyzed

Pair no.	EQ	Acquisition date master image	Acquisition date slave image	Time (JST)	Flight direction	Looking direction	Obs. mode	Incidence angle at scene center (°)	B_p (m)
1	F	November 14, 2014	April 15, 2016	12:53	Des	Left	U-U	32.4	-104
2	M	May 18, 2015	April 18, 2016	00:25	Asc	Right	U-U	50.9	+175
3	M	March 07, 2016	April 18, 2016	12:18	Des	Right	U-U	36.3	-124
4	M	February 10, 2015	April 19, 2016	00:46	Asc	Right	V-V	65.9	+54
5	M	January 26, 2016	April 19, 2016	23:30	Asc	Left	W-W	43.6	-186
6	M	January 14, 2015	April 20, 2016	12:59	Des	Left	U-U	43.0	-3
7	M	December 04, 2015	April 22, 2016	00:11	Asc	Right	H-H	34.0	-147
8	M	March 30, 2016	April 27, 2016	00:18	Asc	Right	U-U	43.0	-228
9	M	April 15, 2016	April 29, 2016	12:52	Des	Left	U-U	32.5	-152
10	M	April 15, 2016	April 29, 2016	23:44	Asc	Left	U-U	24.5	+195
11	A	April 17, 2016	May 01, 2016	0:04	Asc	Right	U-U	20.1	-171
12	A	April 17, 2016	May 01, 2016	11:57	Des	Right	U-U	60.1	+89
13	A	April 18, 2016	May 02, 2016	12:18	Des	Right	U-U	36.3	+87
14	A	April 22, 2016	May 06, 2016	00:11	Asc	Right	H-H	34.0	+55
15	A	April 27, 2016	May 11, 2016	00:18	Asc	Right	U-U	43.0	+362
16	A	May 02, 2016	May 16, 2016	12:18	Des	Right	U-U	36.3	+157

Letters in column EQ represent interferograms that include F: before the main shock (April 16, 2016, M_w 7.0), foreshocks only; M: the date of the main shock; and A: after the main shock only. Des and Asc stand for descending and ascending orbits, respectively. Letters H, U, V and W indicate Stripmap (6 m resolution), Stripmap (3 m resolution), ScanSAR (490 km swath) and ScanSAR (350 km swath) modes, respectively

B_p perpendicular baseline

Additional file 1: Figure A 1a). Therefore, the ruptures most probably appeared after the main shock (M_w 7.0), which occurred on April 16 at 1:25 a.m. (JST) (JMA 2016b).

2. The lengths of the linear surface ruptures are more than several hundreds of meters, and the typical length is several km. Differences in displacement between each side of the ruptures vary from several centimeters to tens of centimeters. Some ruptures are apparent on the ground; however, they are not continuous cracks but many separated crack sections visible in the aerial photographs (Nakano et al. 2016).
3. Within each area the linear surface ruptures have similar features, such as strike and dip direction, and can be divided into several groups (Fig. 2a). For example, in the northwest of the outer rim of Aso caldera, there is a high concentration of parallel ruptures with a WNW–ESE strike showing dip-slip displacement. This shows that the same mechanism was responsible for this group of linear surface ruptures.
4. The strike direction of the ruptures generally coincides with known active faults such as those of the Futagawa and Hinagu fault zones or their conjugate faults (Fig. 2a). Hence, surface rupture generation is closely related to the regional tectonic stress field.
5. As well as the linear surface ruptures, we found numerous surface features caused by strong motion,

such as landslides. Furthermore, in the western Kumamoto city, on the quaternary volcano Mount Kimpo, several ruptures approximately 1 km in length are visible on the volcanic cones. Interestingly, one of the ruptures on Mount Ohagi appeared between April 18 and April 22; therefore, the rupture was possibly caused by an aftershock. Epicenters of the aftershocks are shown in Fig. 2b. In addition, on an alluvial plain of Kumamoto city, a narrow and winding low coherence zone is found. The area may represent the trace of an old river where liquefaction of the ground occurred due to the strong seismic motions.

Features of surface rupture groups

We divided the linear surface ruptures into several groups (Fig. 2a) according to their properties and locations, as follows:

1. Northeast of Aso volcano

There are several parallel linear surface ruptures on the northeastern outer rim of Aso caldera and in the eastern part of Aso valley (Fig. 4). The ruptures in this area run from northeast to southwest. The length of each rupture is predominantly 3 km–5 km, the horizontal spacing between each rupture is approximately 500 m–1 km, and the displacements are at most 10 cm. Dip-slip displacements, where

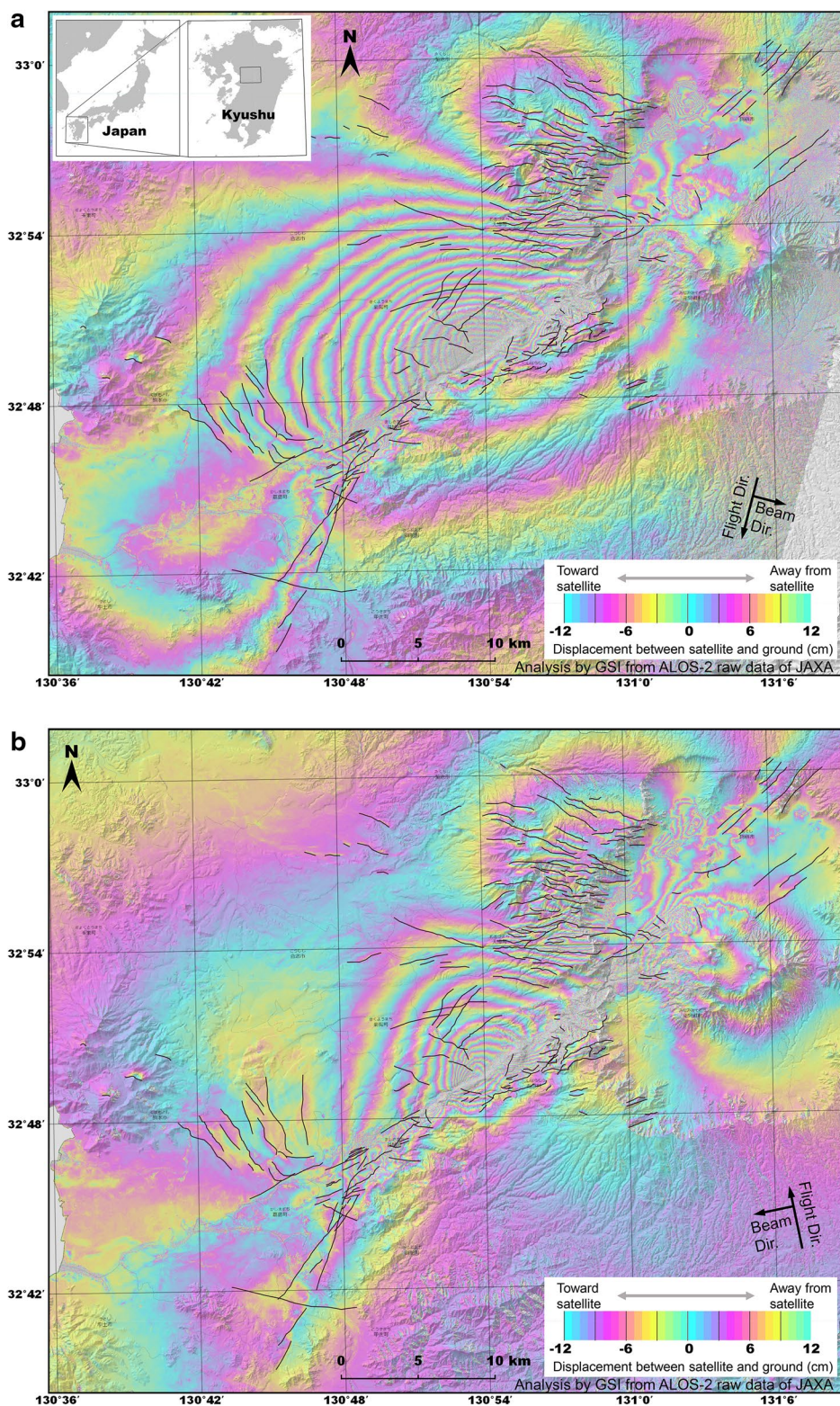


Fig. 1 Typical SAR interferograms used in this study. Solid small lines show the identified linear surface ruptures. **a** ALOS-2 image pair is no. 9 in Table 1. Location of this figure is shown in inset. **b** ALOS-2 image pair is no. 10 in Table 1

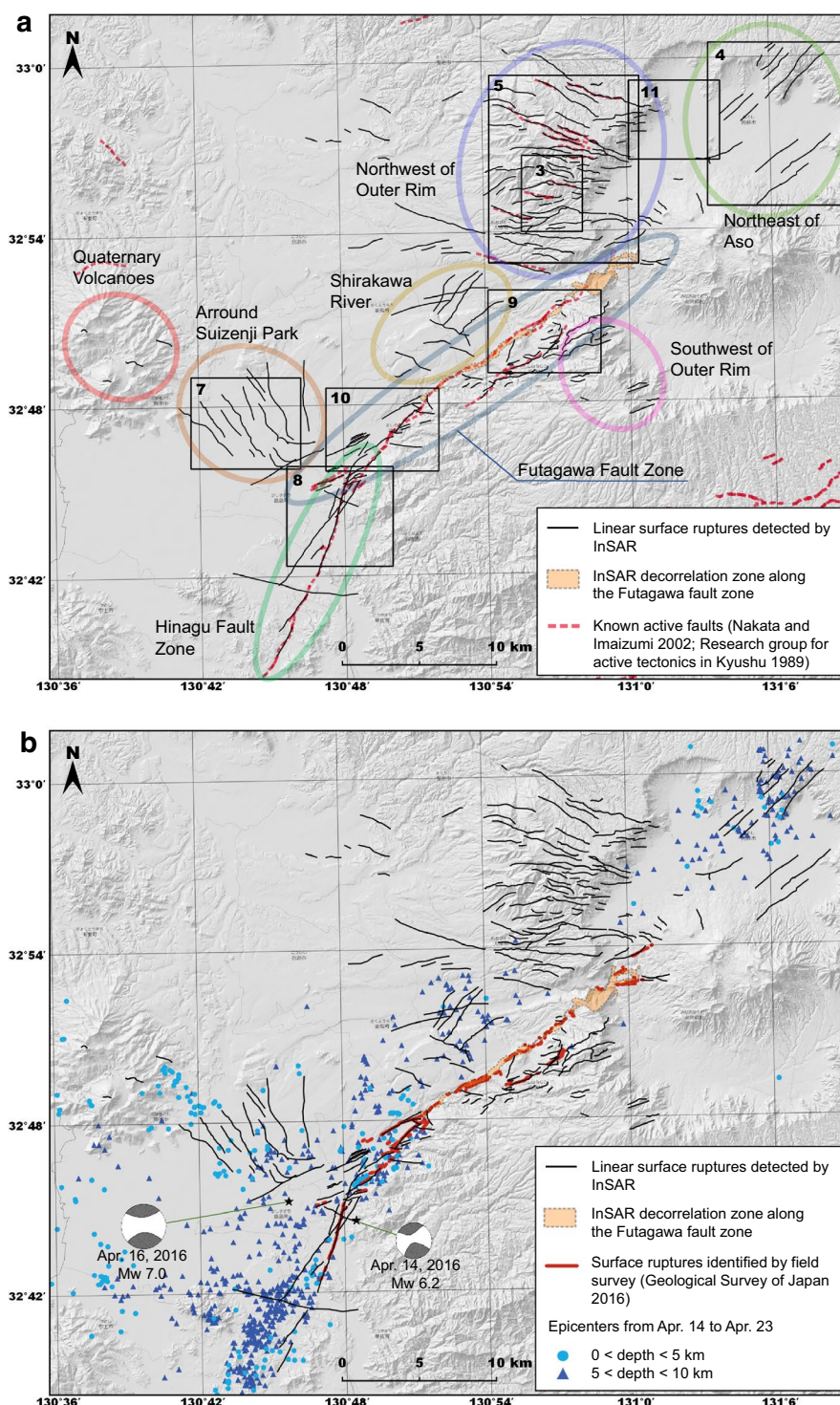


Fig. 2 Identified linear surface ruptures. **a** Small solid lines show identified linear surface ruptures. Numbers correspond to the number of each figure shown later, and the rectangle with the number shows the area of each figure. Red dashed lines show known active faults (Nakata and Imaizumi 2002; Research group for active tectonics in Kyushu 1989). Long, narrow orange area shows the InSAR decorrelation zone along the Futagawa fault zone. Ellipses approximate the areas of each linear surface rupture group classified by location and features. **b** Small solid lines show identified linear surface ruptures. Long, narrow orange area shows the InSAR decorrelation zone along the Futagawa fault zone. Small circles and triangles show epicenters from April 14 to April 23, and beach ball diagrams are from JMA (2016a, b). Red lines show surface ruptures identified by field survey (Geological Survey of Japan 2016)

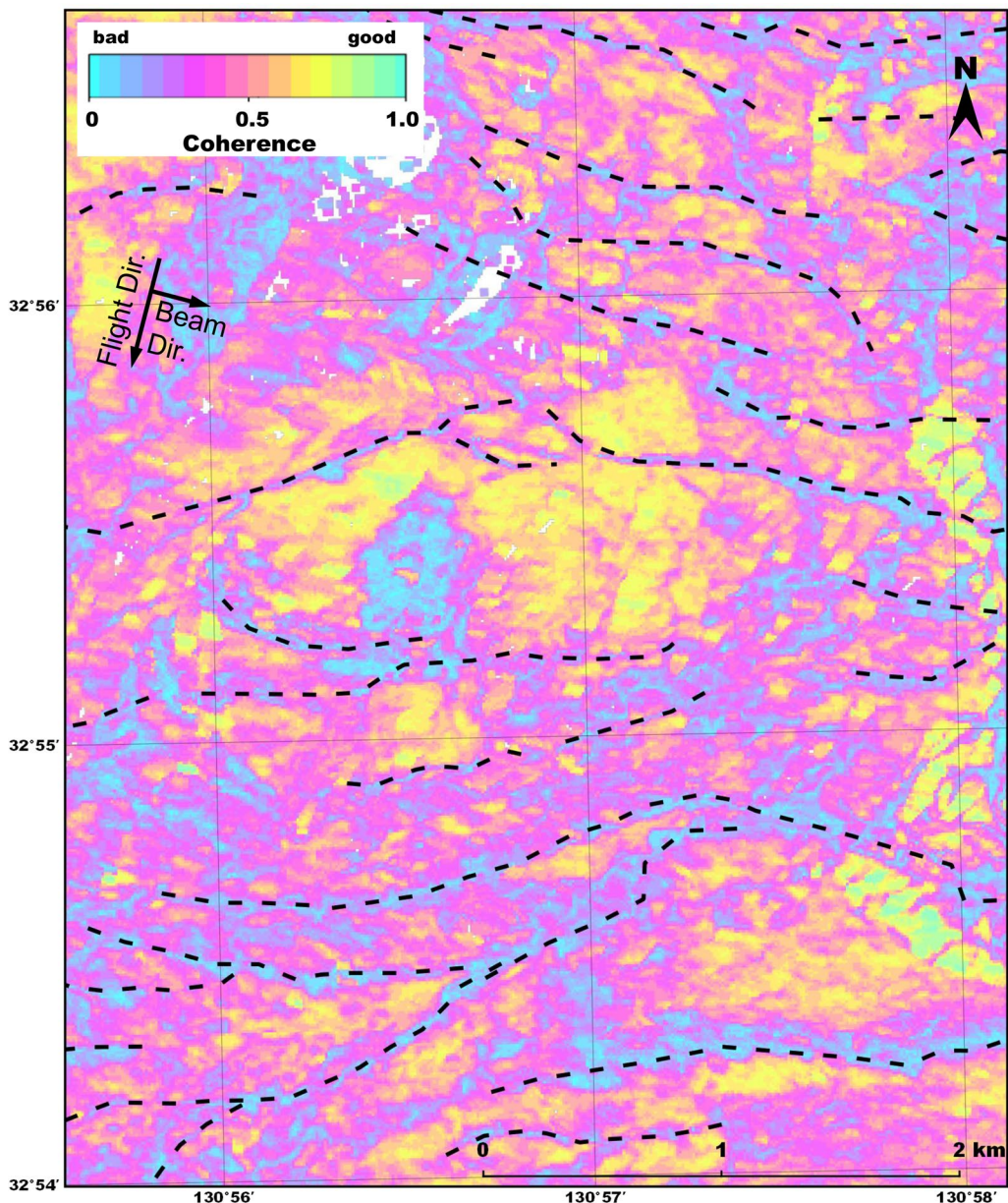


Fig. 3 Coherence map of an interferogram. ALOS-2 image pair is no. 9 in Table 1. Dashed lines show the identified linear surface ruptures. The area is shown in Fig. 2a

the northwestern side moves downward, are generally found in this area. Right-lateral displacements are found on the caldera rim and in the northern Aso valley, and left-lateral displacements are found in the southern Aso valley. These linear surface ruptures are located away from the epicenter of the main shock (JMA 2016b); however, they appear in the northeastern extension of the Futagawa fault zone where aftershocks were recorded near to the

rupture locations (Fig. 2b). No conjugate linear surface ruptures are observed in this area.

2. Northwest of outer rim of Aso caldera

Several dozens of linear surface ruptures are found in the area northwest of the outer rim of Aso caldera (Figs. 2, 5). In this group, the ruptures generally have a WNW–ESE direction and typical dip-slip displacements. To visualize and clarify the displacement, we conducted a three-dimensional (3-D)

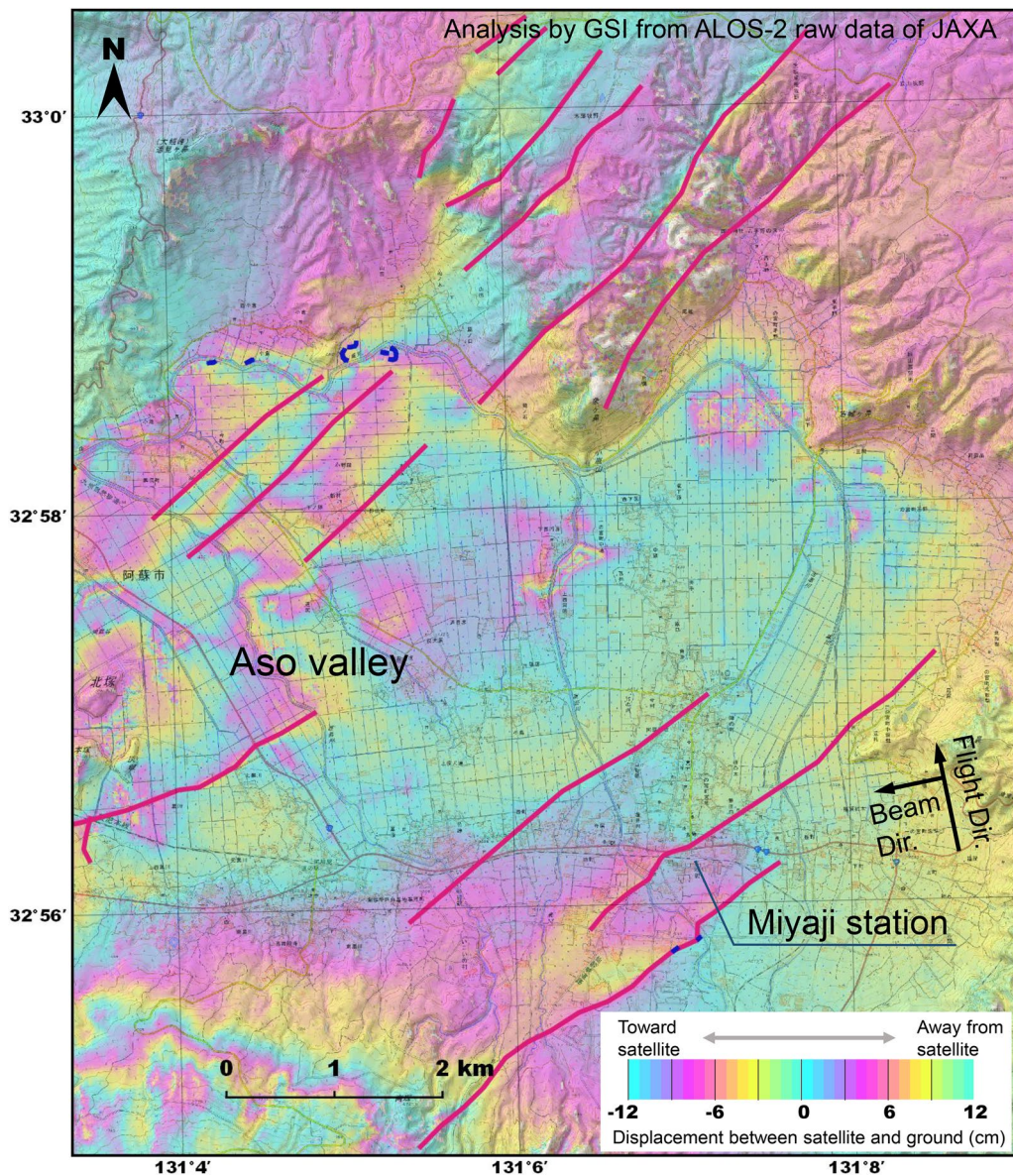


Fig. 4 Linear surface ruptures northeast of Aso volcano. ALOS-2 image pair is no. 10 in Table 1. Red solid lines show the identified linear surface ruptures. Blue dots show surface cracks interpreted from aerial photographs (Nakano et al. 2016). The area is shown in Fig. 2a

analysis (Morishita et al. 2016). Figure 5a shows a high-pass-filtered up-down displacement map using ALOS-2 image pairs 3, 7, 8, 9 and 10 in Table 1 and the identified linear surface ruptures. The largest up-down displacement gap (difference of displacement between both sides of each rupture) of more than 30 cm is found in the southern part of this area. This rupture group is also further divided into two groups, whereby the northwest group mainly shows dip slip where the south side moves downward, and the southeast group mainly shows the north side

moving downward. The group boundary is shown in Fig. 5b. The displacements between adjacent parallel linear surface ruptures gradually change and likely show rupture discontinuity. The displacement is sawtooth in shape, and interestingly, the direction of the sawtooth pattern differs between the two groups. Figure 6 shows a schematic model explaining these sawtooth displacements, consisting of half-graben blocks bounded by the linear surface ruptures and a graben at the center of the model, which is the boundary between the two groups. In

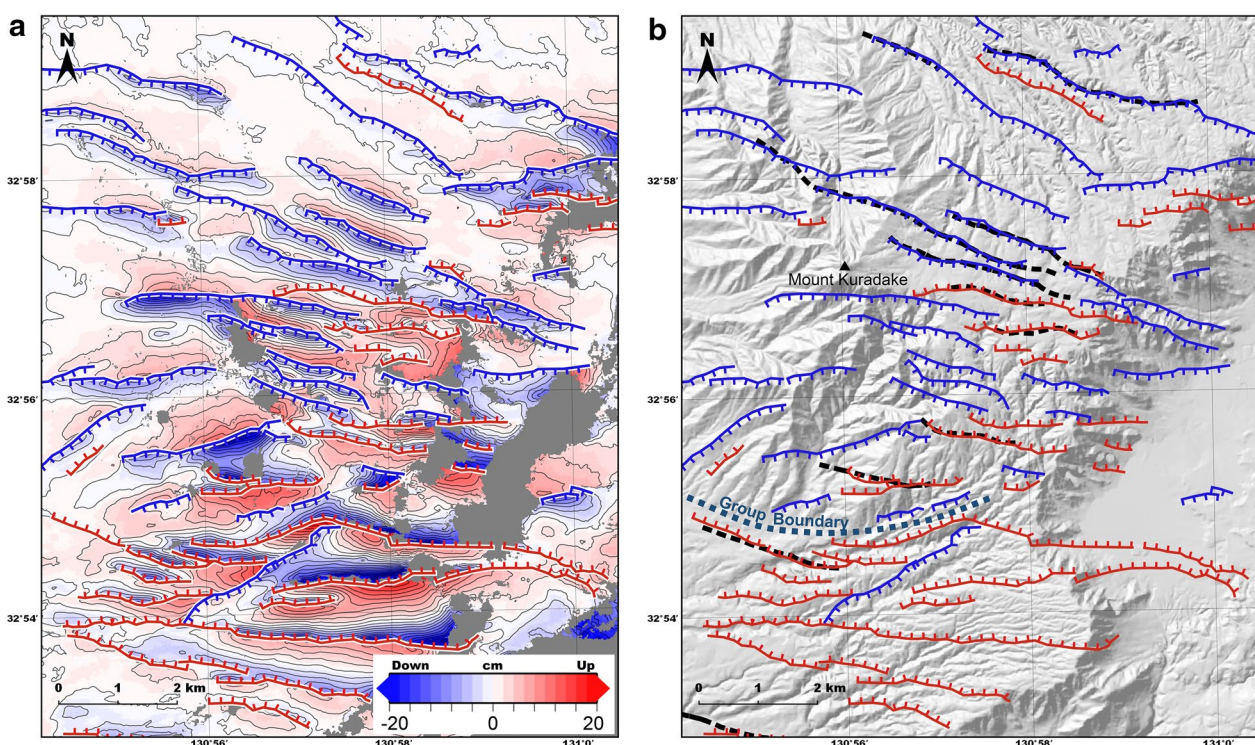


Fig. 5 Linear surface ruptures northwest of the outer rim of Aso caldera. **a** A high-pass-filtered up–down displacement map made by three-dimensional (3-D) analysis (Morishita et al. 2016) using ALOS-2 image pairs 3, 7, 8, 9 and 10 in Table 1. Red and blue areas represent up and down, respectively. The contour interval is 2 cm. Red solid lines show the identified linear surface ruptures with dip slip where the north side moving down, and blue solid lines show the identified linear surface ruptures with dip slip where the south side moving down. Ticks of the lines show the lower side of each displacement. The area is shown in Fig. 2a. **b** Red solid lines show the identified linear surface ruptures with dip slip where the north side moving down, and blue solid lines show the identified linear surface ruptures with dip slip where the south side moving down. Ticks of the lines show the lower side of each displacement. Black dashed lines show known active faults (Nakata and Imaizumi 2002; Research group for active tectonics in Kyushu 1989)

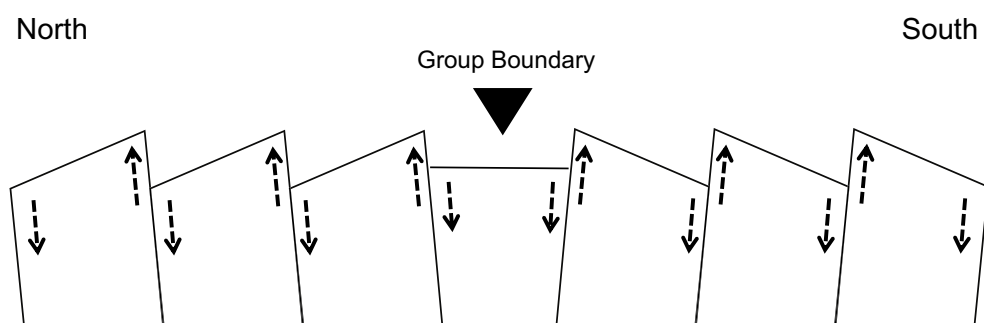


Fig. 6 Schematic explanation of "sawtooth" displacement. Schematic profile of surface displacement from north to south in the northwest area of the outer rim of Aso caldera. Dashed arrows show displacement of each block divided by linear surface ruptures

reality, Fig. 5a shows that the displacement in this graben area is rather complicated, yet nevertheless the graben forms low valleys in this area and the valleys coincide with the group boundary in Fig. 5b. Because there is clear low coherence of the

interferograms along the linear surface ruptures in this area (Fig. 3) compared with other areas, the surface of the ground would tend to break rather than bend. Before the current Aso caldera was formed approximately 70–80 thousand years ago, there were

four large eruptions (Ono and Watanabe 1985), named Aso-1, Aso-2, Aso-3 and Aso-4. Since this area is mainly covered by the associated pyroclastic flow deposits (Ono and Watanabe 1985; Watanabe 1978), the ground is likely to be brittle on the scale of the pixels in the interferograms. There are about ten known active faults in this area, known as the Kuradake fault group, that show graben landforms (Geographical Survey Institute 1994; Nakata and Imaizumi 2002; Research group for active tectonics in Kyushu 1989), and the positions and directions of the linear surface displacements coincide with those of the known active faults (Fig. 5b).

Additionally, in the area southwest of the outer rim of Aso caldera, especially around Mount Tawara (in the southwest of the outer rim in Fig. 2), there are several linear surface ruptures. However, the number is much smaller than that in the northwest of the outer rim and they do not show horizontal rows of half-grabens but a single graben displacement in each location instead.

3. Around Suizenji Park

Near Kumamoto city center, clear linear surface ruptures run from northwest to southeast (Fig. 7a) and Goto et al. (2016) found minor surface breaks around Suizenji Park by field survey. The features of this linear surface rupture group are similar to those in the northwest of the outer rim of Aso caldera group. In this area, dip-slip displacements are dominant and sawtooth displacements are also found. This area is situated in an alluvial plain, and the topography is rather flat. However, Fig. 7b shows that one of the largest displacements to the south of Kengun Shrine coincides well with the topography (a height difference of only several meters). Therefore, some of these linear surface ruptures are likely to be hidden active faults that had moved in the past. The fact that their directions coincide with the conjugate faults of the Futagawa fault zone suggests that this group around Suizenji Park is closely related to activity of the Futagawa fault zone and that they have experienced simultaneous movement many times previously.

4. Hinagu fault zone

The first large earthquake (M_w 6.2) of the 2016 Kumamoto earthquake sequence occurred on April 14, and crustal deformation shows that the cause of the earthquake was movement of the Hinagu fault zone (Yarai et al. 2016). As mentioned above, the linear surface ruptures in Fig. 8 along the Hinagu fault zone likely appeared at the same time as or after the main shock on April 16. Figure 8 also shows that known active faults of the Hinagu fault zone (Nakata and

Imaizumi 2002; Research group for active tectonics in Kyushu 1989) generally coincide with some of the linear surface ruptures; however, there are others, including several parallel and conjugate linear surface ruptures, and even some that meet the known active faults at an angle of approximately 20°. The linear surface ruptures of the Hinagu fault zone mostly show right-lateral and dip-slip displacements. The epicenter of the main shock is very close to this area, but the focal mechanism in Fig. 2b (JMA 2016a, b) and the fault model derived from crustal deformation (Yarai et al. 2016) do not match each other. This mismatch is possibly related to the complex distribution of linear surface ruptures around the Hinagu fault zone.

5. Futagawa fault zone

As mentioned above, crustal deformation (Yarai et al. 2016) and the numerous surface cracks (Nakano et al. 2016) indicate that the Futagawa fault zone was the origin of the main shock. In Nishihara village, in the eastern part of the Futagawa fault zone, there is a heavy decorrelation belt of the interferograms, shown in Figs. 2 and 9. Figure 9 shows that the decorrelation belt coincides with the northern margin of the Futagawa fault zone. A fault model simulation using crustal deformation (Yarai et al. 2016) shows that the largest fault motion occurred in this area, suggesting that the large fault motion of the main shock almost certainly generated this decorrelation belt. The high linearity of the decorrelation belt and high concentration of surface cracks in aerial photographs (Nakano et al. 2016) also support this. Several linear surface ruptures run parallel to the south of the belt (Fig. 9). Deformation in the area between the decorrelation belt and the southern parallel linear surface rupture group is divided into several block movements. The movements are larger than those of the surrounding area and show a very complicated geographical distribution. These displacements indicate the existence of a subfault system that branches off from the main earthquake fault. The southern parallel linear surface ruptures likely consist of the subfault system of the main earthquake fault, and the blocks moved in a complicated manner (Toda et al. 2016). The subfault system contains a known active fault, named the Idenokuchi fault (Research group for active tectonics in Kyushu 1989); however, the observed linear surface ruptures and the displacements indicate the existence of a more complicated subfault system than previously mapped.

6. Mashiki town

Mashiki town is situated at the junction of the Futagawa fault zone and the Hinagu fault zone. In the

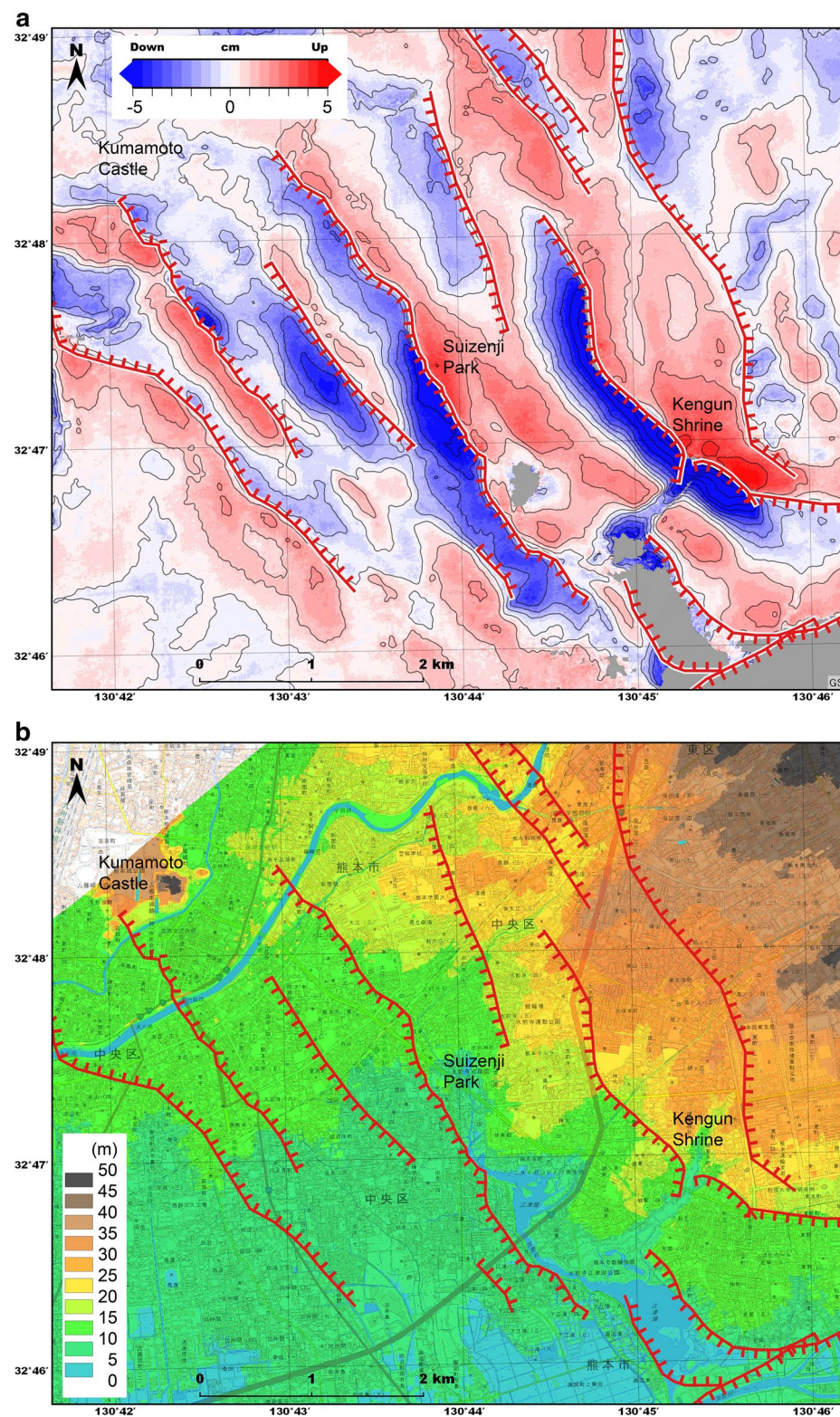


Fig. 7 Linear surface ruptures around Suizenji Park, Kumamoto city center. **a** A high-pass-filtered up–down displacement map made by three-dimensional (3-D) analysis (Morishita et al. 2016) using ALOS-2 image pairs 3, 8, 9 and 10 in Table 1. Red and blue areas represent up and down, respectively. The contour interval is 1 cm. Red solid lines show the identified linear surface ruptures. Ticks of the red lines show the lower side of each displacement. The area is shown in Fig. 2a. **b** Red solid lines show the identified linear surface ruptures. Ticks of the red lines show the lower side of each displacement. Topography is drawn using a DEM

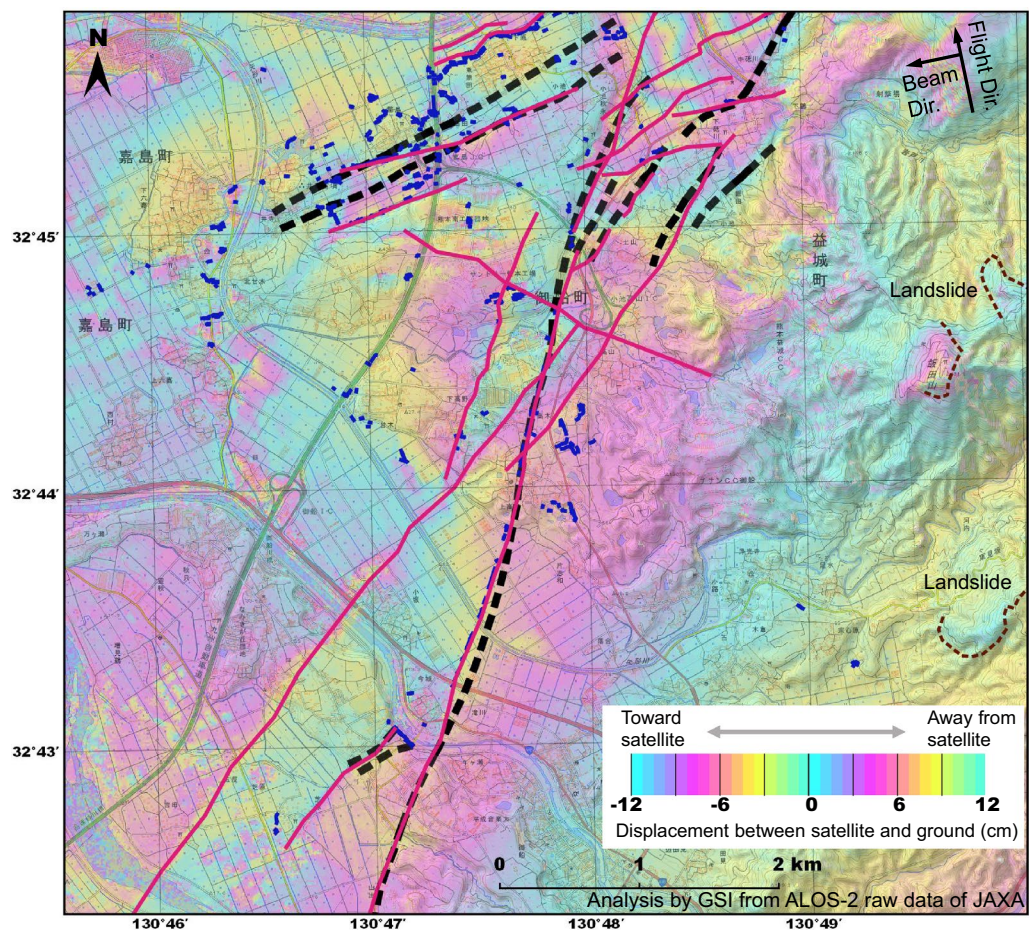


Fig. 8 Linear surface ruptures along the Hinagu fault zone. ALOS-2 image pair is no. 10 in Table 1. Red solid lines show the identified linear surface ruptures. Blue dots show surface cracks interpreted from aerial photographs (Nakano et al. 2016). Black dashed lines show known active faults (Nakata and Imaizumi 2002; Research group for active tectonics in Kyushu 1989). Brown dashed lines show boundaries of the identified landslides. The area is shown in Fig. 2a

downtown of Mashiki town, the structural damage was so heavy that even new and reinforced houses that met the earthquake resistance standards of the Building Standard Law were also damaged (Kawase et al. 2016). This area is on the western extension line of the Futagawa fault zone (Fig. 2); however, the interferograms of the downtown area are heavily decorrelated, so we were unable to find any linear surface ruptures or displacements (Fig. 10). The heavy decorrelation area shown in Fig. 10 coincides with the structural damage area (Kawase et al. 2016) where ground motion of the earthquakes would have been very strong. There is a paddy field on the southern side of the downtown area, and several linear surface ruptures are found in this paddy field (Fig. 10). At this time, there is no apparent evidence

for the relationship between these ruptures and the strong seismic motions.

Conversely, in the eastern part of Mashiki town, the coherence of the interferograms is good and several linear surface ruptures are mapped (Fig. 10). It is interesting that large and clear cracks are found in this area using the aerial photographs (Nakano et al. 2016) yet coherence is maintained. This may suggest that linear surface ruptures in this area appeared very smoothly and without disorderly movement.

7. Uchinomaki

Large deformation is concentrated in Aso valley along the northwest outer rim of Aso caldera. Figure 11 shows a close-up interferogram of the northern part of this deformation. The diameter of the deformed area is approximately 2 km, and hori-

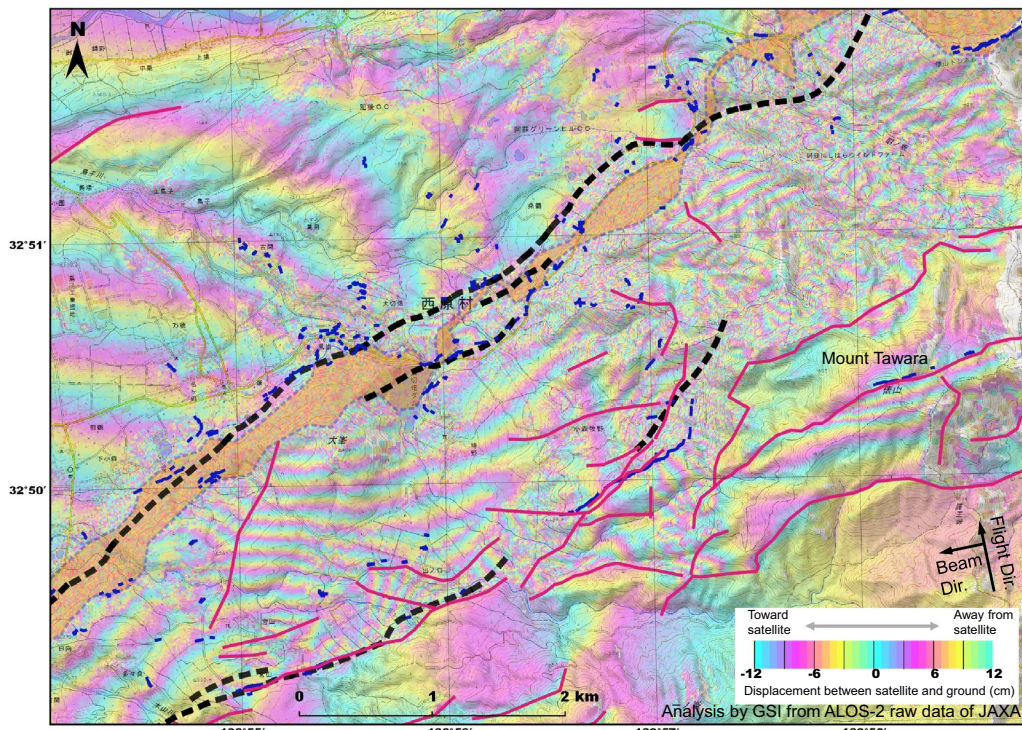


Fig. 9 Linear surface ruptures along the Futagawa fault zone. ALOS-2 image pair is no. 10 in Table 1. Red solid lines show the identified linear surface ruptures. Blue dots show surface cracks interpreted from aerial photographs (Nakano et al. 2016). Black dashed lines show known active faults (Nakata and Imaizumi 2002; Research group for active tectonics in Kyushu 1989). Long, narrow orange area shows the InSAR decorrelation zone along the Futagawa fault zone. The area is shown in Fig. 2a

zontal displacement in a NNW direction of more than 2 m is found in the central area, around Uchinomaki hot spring. Significant deformation is only found within the deformation area; the northwest boundary almost coincides with the caldera rim (Fig. 11), and the deformation resembles a landslide or fluid flow in a bowl. In the southern part of the largest displacement, graben-like surface cracks are seen in aerial photographs (Nakano et al. 2016), also shown in Fig. 11. We suggest that the deformation and graben-like cracks are not linear surface ruptures caused by tectonic forces for the following reasons. Firstly, the displacements do not show horizontal linearity. Each surface crack has a maximum length of several hundred meters; however, the interferograms show that the group of surface cracks does not have a straight-line configuration. Secondly, displacements outside of the deformation area are not found. If the displacements were caused by tectonic forces, displacements should also be found on both sides of the linear surface ruptures. The inside of the area with the graben-like surface cracks shows low coherence in the interferograms, and therefore, the cracks were likely caused by

surface tension due to large horizontal deformation. About 9000 years ago, there was a lake in the western Aso valley and a lake bottom deposit about 50 m thick was found at a boring site in the southern part of Uchinomaki (Hase et al. 2010). We suggest that soils in this area are wet and liquefaction due to strong ground motions caused large deformation in the form of lateral flow.

8. Post-seismic deformation

Figure 12 shows post-seismic deformation and the linear surface ruptures found in this study. The displacements are <10 cm, and almost all show subsidence. Major post-seismic deformation is found along the Futagawa fault zone, especially at the junction of the Futagawa and Hinagu fault zones. Interestingly, clear post-seismic deformation is found in the area around Suizenji Park, whereas no post-seismic deformation is found in and around the outer rim of Aso caldera. There were many aftershocks around Suizenji Park, yet almost no aftershocks around the outer rim of Aso caldera (Fig. 2b). Both the Suizenji Park area and the outer rim show graben motion, but the post-seismic displacements in the Suizenji Park area show that some form of deformation

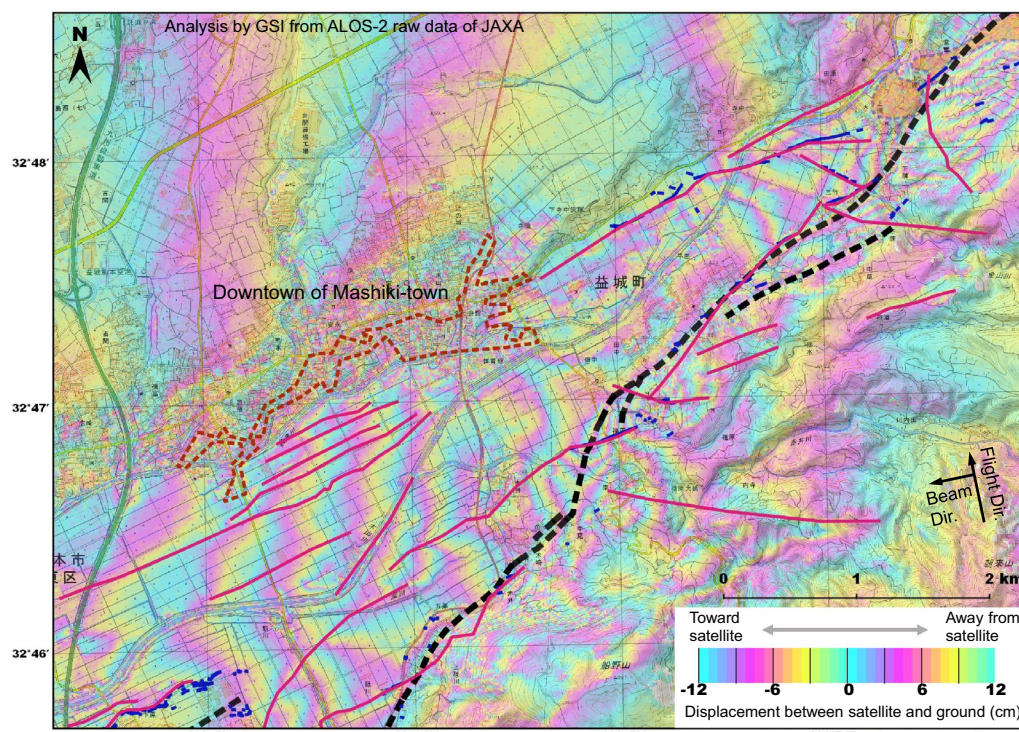


Fig. 10 Linear surface ruptures around Mashiki town. ALOS-2 image pair is no. 10 in Table 1. Red solid lines show the identified linear surface ruptures. Blue dots show surface cracks interpreted from aerial photographs (Nakano et al. 2016). Black dashed lines show known active faults (Nakata and Imaizumi 2002; Research group for active tectonics in Kyushu 1989). Area surrounded by brown dashed line shows the InSAR decorrelation zone in downtown of Mashiki town. Orange area in the northeast of this figure shows the InSAR decorrelation zone along the Futagawa fault zone. The area is shown in Fig. 2a

mechanism was still active after the main shock. This evidence suggests a close relationship between the Suizenji Park area and the Futagawa fault zone. Clear post-seismic deformation is also found along a long linear surface rupture in Ozu town running WNW–ESE (Fig. 12b).

Discussion

The majority of linear surface ruptures found in this study, except for those along the Futagawa and Hinagu fault zones, do not have a direct connection to the main earthquake fault system because there is a clear geographical distance between the main earthquake faults and the linear surface ruptures. Therefore, motion on linear surface ruptures is likely to release secondary stress caused by the main fault system and/or the strong seismic motion. In other words, slip on the linear surface ruptures was triggered by the main earthquake or aftershocks. Since some ruptures are recognized as known active faults from their geologic features, these are certainly preexisting geologically weak surfaces that moved co-seismically and/or post-seismically. We propose a hypothesis whereby similar linear surface rupture

movement occurred many times throughout geologic history and formed these features. This relationship between linear surface ruptures and topography was also found in previous studies (Fujiwara et al. 2000a, b). Each displacement of the ruptures would have been small; however, once enough slip had accumulated, the landform would then be recognized as an active fault. Fujiwara et al. (2000a, b) reported that displacement of linear surface ruptures is closely related to topography, but in this study, the relationship between displacement of secondary linear surface ruptures and topography is rather weak. We suggest that one reason is the volcanic activity of Aso volcano, including pyroclastic flows, ash and lava, which covered older displacements of the ruptures. This can also explain why there are many more linear surface ruptures visible in the earthquake sequence than known active faults.

A question remains as to whether the secondary linear surface ruptures will become “primary” earthquake faults in the future. We have no concrete answer to this question; however, it is nevertheless important to prepare for strong future seismicity along the linear surface ruptures because Fujiwara et al. (2000b) suggested that these

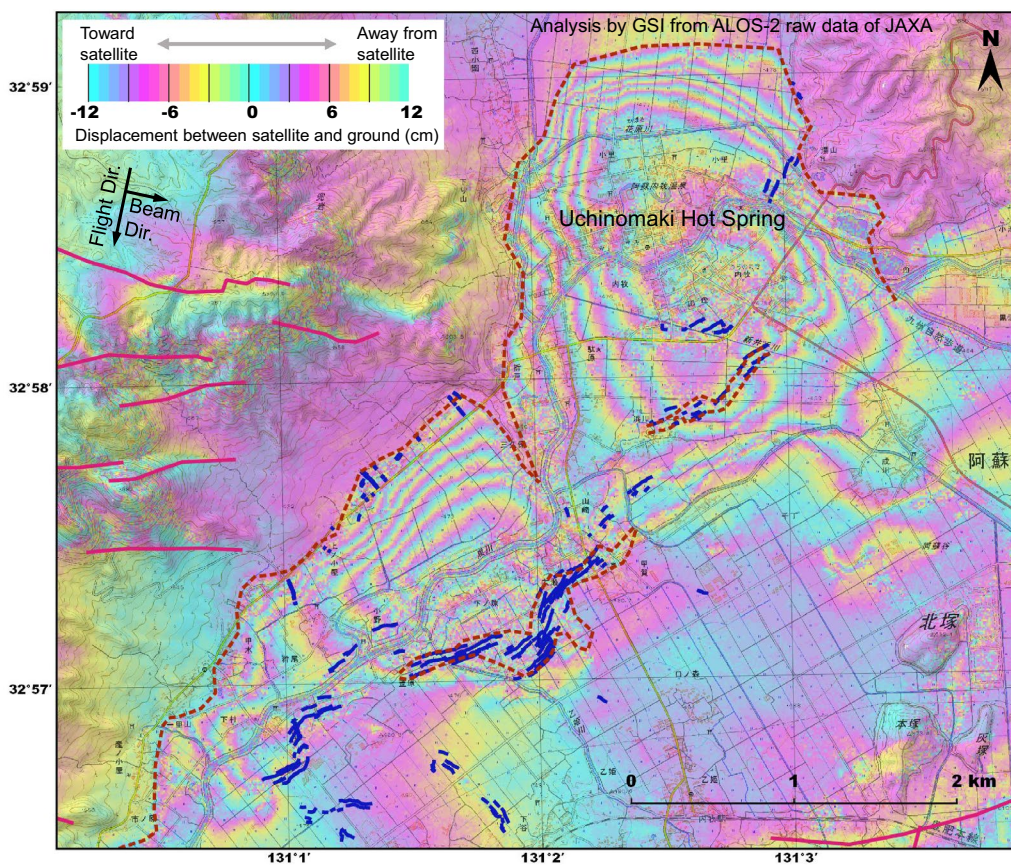


Fig. 11 Large deformation in and around Uchinomaki hot spring. ALOS-2 image pair is no. 9 in Table 1. Red solid lines show the identified linear surface ruptures. Blue dots show surface cracks interpreted from aerial photographs (Nakano et al. 2016). Brown dashed lines show boundaries of the large deformation or heavy decorrelation of the interferograms. The area is shown in Fig. 2a

secondary ruptures locally accelerated the main seismic motion.

The trigger for these linear surface ruptures is most likely to be local tectonic stress, and their geographical distribution is also probably related to the tectonic stress field. The tectonic stress field of the graben groups, such as around Aso caldera and Suizenji Park, appears simple because the distribution of linear surface ruptures and displacements are rather uniform compared with those of the main earthquake faults. Regarding these groups, the displacement of each rupture tends to be located close to the linear surface rupture (e.g., Figs. 4, 5, 7). If a linear surface rupture has a deep structure (e.g., several km depth) and the deeper part moves, the observed displacement would appear in a horizontally wide area of several kilometers. However, large displacement over a wide area is found only along the main earthquake faults: the Futagawa and Hinagu fault zones. Moreover, the situation of the linear surface ruptures in and around the Futagawa and Hinagu fault zones is very complicated. To understand the complex linear surface ruptures along

the Futagawa and Hinagu fault zones as well as the complete earthquake sequence, further study using not only crustal deformation but a combination of other tools, such as seismic wave analysis, would be required.

Conclusions

Using InSAR measurements, we mapped approximately 230 linear surface ruptures with small displacements in the 2016 Kumamoto earthquake sequence. The existence of these linear surface ruptures is key to understanding the geographical distribution of seismicity and regional stress fields.

1. The linear surface ruptures are found not only along the main earthquake faults, the Futagawa and Hinagu fault zones, but also in areas away from the main faults, such as around Aso caldera and in Kumamoto city center. Slips on the latter are probably triggered by the main earthquake or aftershocks.
2. The typical length of the linear surface ruptures is several kilometers. In each area, the linear surface ruptures

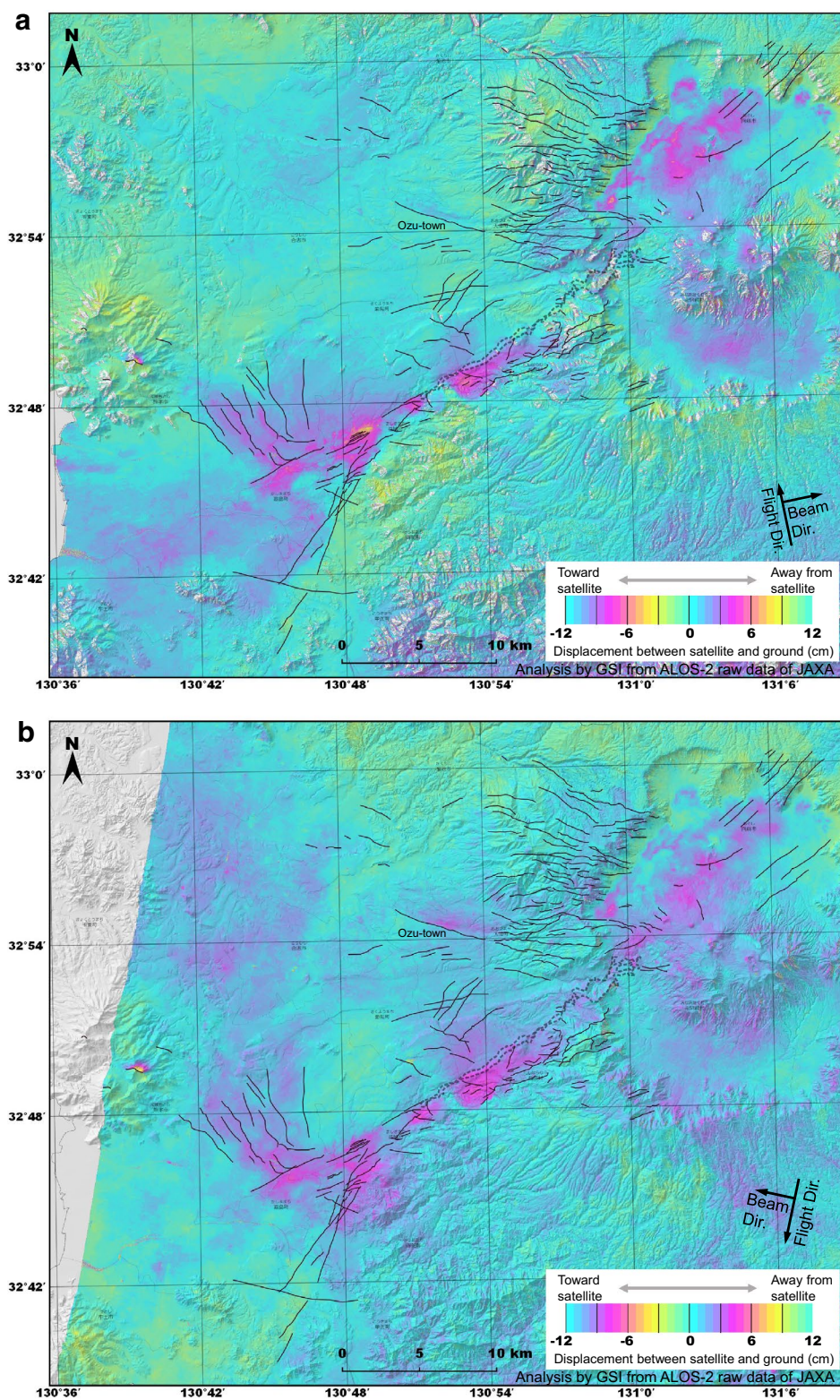


Fig. 12 Interferograms showing post-seismic deformation. **a** ALOS-2 image pair is no. 11 in Table 1. Solid small lines show the identified linear surface ruptures in this study. Long, narrow area surrounded by a dashed line shows the InSAR decorrelation zone found in this study along the Futagawa fault zone. **b** ALOS-2 image pair is no. 13 in Table 1. Solid small lines show the identified linear surface ruptures in this study. Long, narrow area surrounded by a dashed line shows the InSAR decorrelation zone found in this study along the Futagawa fault zone

- tend to run parallel each other and at almost the same horizontal spacing. They are therefore divided into several groups based on their locations and features.
3. Many secondary linear surface ruptures show graben or half-graben displacements, and some of the displacements are related to existing topography. This fact suggests that the local tectonic stress field was responsible for the secondary linear surface ruptures.
 4. The position of some linear surface ruptures is found to coincide with known active faults, as indicated by geologic features (e.g., Figs. 5b, 8, 9, 10); however, there are many more linear surface ruptures than known active faults.
 5. InSAR from space is a powerful tool to detect linear surface ruptures with small displacements. However, since the majority of ruptures do not exist on the ground as a continuous crack, it would be difficult to fully comprehend linear surface rupture characteristics using only ground surveys or aerial photographs.
 6. A long and narrow decorrelation zone of the interferograms exists from Mashiki town to Nishihara village along the Futagawa fault zone (Figs. 2, 9). In the decorrelation zone, each scatter of the ground SAR target pixel (horizontal spacing is several meters or more) moved randomly and/or with a high interferogram fringe rate due to the main fault movement and associated strong seismicity.

Additional file

Additional file 1: Figure A. Interferograms used in this study and identified linear surface ruptures. Figure numbers correspond to the number of the ALOS-2 image pair in Table 1.

Authors' contributions

SF mapped the linear surface ruptures and drafted the manuscript. HY, TK and YM analyzed the interferograms. TN and HUn constructed aerial photograph data, and they and TK conducted field surveys. BM, HN, YMi, HUe and YK constructed the interferograms and other supporting data. All authors read and approved the final manuscript.

Acknowledgements

ALOS-2 data were provided from the Earthquake Working Group under a cooperative research contract with JAXA. The ownership of ALOS-2 data belongs to JAXA.

Competing interests

The authors declare that they have no competing interests.

Received: 29 June 2016 Accepted: 6 September 2016

Published online: 26 September 2016

References

- Fujiwara S, Tobita M (1999) SAR interferometry techniques for precise surface change detection. *J Geod Soc Jpn* 45:283–295 (**in Japanese with English abstract**)
- Fujiwara S, Rosen PA, Tobita M, Murakami M (1998) Crustal deformation measurements using repeat-pass JERS 1 synthetic aperture radar interferometry near the Izu Peninsula, Japan. *J Geophys Res* 103:2411–2426. doi:[10.1029/97JB02382](https://doi.org/10.1029/97JB02382)
- Fujiwara S, Tobita M, Murakami M, Nakagawa H, Rosen PA (1999) Baseline determination and correction of atmospheric delay induced by topography of SAR interferometry for precise surface change detection. *J Geod Soc Jpn* 45:315–325 (**in Japanese with English abstract**)
- Fujiwara S, Nishimura T, Murakami M, Nakagawa H, Tobita M, Rosen PA (2000a) 2.5-D surface deformation of M6.1 earthquake near Mt Iwate detected by SAR interferometry. *Geophys Res Lett* 27:2049–2052. doi:[10.1029/1999GL011291](https://doi.org/10.1029/1999GL011291)
- Fujiwara S, Ozawa S, Murakami M, Tobita M (2000b) Estimation of fault positions of the 1995 Hyogo-ken nanbu earthquake using surface displacement gradient detected by SAR interferometry. *J Seismol Soc Jpn* 53:127–136 (**in Japanese with English abstract**)
- Fukushima Y, Takada Y, Hashimoto M (2013) Complex ruptures of the 11 April 2011 Mw 6.6 Iwaki earthquake triggered by the 11 March 2011 Mw 9.0 Tohoku earthquake, Japan. *Bull Seismol Soc Am* 103:1572–1583. doi:[10.1785/0120120140](https://doi.org/10.1785/0120120140)
- Geographical Survey Institute (1994) Asosan. 1:30,000 Land condition map of volcano. Geographical Survey Institute, Tsukuba (**in Japanese with English abstract**)
- Geological Survey of Japan (2016) Surface earthquake faults associated with the 2016 Kumamoto earthquake. <https://www.gsj.jp/hazards/earthquake/kumamoto2016/kumamoto20160513-1.html>. Accessed 10 Aug 2016 (**in Japanese**)
- Geospatial Information Authority of Japan (2014) Overview and types of digital elevation model of fundamental geospatial data. <http://fgd.gsi.go.jp/download/DEMkind.htm>. Accessed 10 Aug 2016 (**in Japanese**)
- Geospatial Information Authority of Japan (2016) 2016 Kumamoto earthquake, detection of deformation using ALOS-2 SAR interferometry. <http://www.gsi.go.jp/BOUSA/H27-kumamoto-earthquake-index.html#3>. Accessed 6 June 2016 (**in Japanese**)
- Goto H, Kumahara Y, Nakata T, Ishiguro S, Ishimura D, Ishiyama T, Okada S, Kagohara K, Kashihara S, Kaneda H, Sugito N, Suzuki Y, Takenami D, Tanaka K, Tanaka T, Tsutsumi H, Toda S, Hirouchi D, Matsuta N, Moriki H, Yoshida H, Watanabe M (2016) Surface fault ruptures of the 2016 Kumamoto Earthquake. In: Paper presented at the Japan Geoscience Union meeting, Chiba, Japan, 22–26 May 2016 (MIS34-P44)
- Guerrieri L, Baer G, Hamiel Y, Amit R, Blumetti AM, Comerci V, Di Manna P, Michetti AM, Salamon A, Mushkin A, Sileo G, Vittori E (2010) InSAR data as a field guide for mapping minor earthquake surface ruptures: ground displacements along the Paganica Fault during the 6 April 2009 L'Aquila earthquake. *J Geophys Res* 115:B12331. doi:[10.1029/2010JB007579](https://doi.org/10.1029/2010JB007579)
- Hanssen R (2001) Radar interferometry: data interpretation and error analysis. Kluwer, Dordrecht
- Hase Y, Miyabuchi Y, Haruta N, Sasaki N, Yumoto T (2010) Change of sedimentary facies and topographic process after the late period of the Last Glacial Age of Asodani in the northern area of Aso Caldera in Central Kyushu, Japan. *Bull Goshoura Cret Mus* 11:1–10 (**in Japanese with English abstract**)
- Japan Meteorological Agency (2016a) CMT solution (April 2016). <http://www.data.jma.go.jp/svd/eqev/data/mech/cmt/cmt201604.html>. Accessed 6 June 2016 (**in Japanese**)
- Japan Meteorological Agency (2016b) Hypocenter map (2016 Kumamoto earthquake). http://www.data.jma.go.jp/svd/eqev/data/2016_04_14_kumamoto/kouiki.pdf. Accessed 6 June 2016 (**in Japanese**)
- Kawase H, Matsushima S, Nagashima F, Bao Y (2016) The cause of heavy damage concentration in downtown Mashiki-cho inferred from observed data and field survey. In: Paper presented at the Japan Geoscience Union meeting, Chiba, Japan, 22–26 May 2016 (MIS34-08)
- Kobayashi T, Tobita M, Nishimura T, Suzuki A, Noguchi Y, Yamanaka M (2011) Crustal deformation map for the 2011 off the Pacific coast of Tohoku Earthquake, detected by InSAR analysis combined with GEONET data. *Earth Planets Space* 63:621–625. doi:[10.5047/eps.2011.06.043](https://doi.org/10.5047/eps.2011.06.043)
- Kumahara Y, Goto H, Nakata T, Ishiguro S, Ishimura D, Ishiyama T, Okada S, Kagohara K, Kashihara S, Kaneda H, Sugito N, Suzuki Y, Takenami D, Tanaka K, Tanaka T, Tsutsumi H, Toda S, Hirouchi D, Matsuta N, Mita T, Moriki H, Yoshida H, Watanabe M (2016) Distribution of surface rupture associated with the 2016 Kumamoto earthquake and its significance. In: Paper presented at the Japan Geoscience Union meeting, Chiba, Japan, 22–26 May 2016 (MIS34-05)

- Morishita Y, Kobayashi T, Yarai H (2016) Three-dimensional deformation mapping of a dike intrusion event in Sakurajima in 2015 by exploiting the right- and left-looking ALOS-2 InSAR. *Geophys Res Lett* 43:4197–4204. doi:10.1002/2016GL068293
- Nakano T, Une H, Sekiguchi T, Sakai H, Yoshida K (2016) Distribution of surface cracks caused by the 2016 Kumamoto Earthquake interpreted from aerial photos. In: Paper presented at the Japan Geoscience Union meeting, Chiba, Japan, 22–26 May 2016 (MIS34-P55)
- Nakata T, Imaizumi T (eds) (2002) Digital active fault map of Japan. University of Tokyo Press, Tokyo
- Nishimura T, Tobita M, Yarai H, Amagai T, Fujiwara M, Une H, Koarai M (2008) Episodic growth of fault-related fold in northern Japan observed by SAR interferometry. *Geophys Res Lett.* doi:10.1029/2008GL034337
- Ono K, Watanabe K (1985) Geological map of Aso Volcano. Geological map of volcanoes. Geological Survey of Japan, Tsukuba
- Oskin ME, Arrowsmith JR, Corona AH, Elliot AJ, Fletcher JM, Fielding EJ, Gold PO, Garcia JJJ, Hudnut KW, Liu-Zeng J, Teran OJ (2012) Near-field deformation from the El Mayor-Cucapah earthquake revealed by differential LiDAR. *Science* 335:702–705. doi:10.1126/science.1213778
- Price EJ, Sandwell DT (1998) Small-scale deformations associated with the 1992 Landers, California, earthquake mapped by synthetic aperture radar interferometry phase gradients. *J Geophys Res* 103:27001–27016. doi:10.1029/98JB01821
- Research group for active tectonics in Kyushu (1989) Active tectonics in Kyushu. University of Tokyo Press, Tokyo (in Japanese)
- Shirahama Y, Yoshimi M, Awata Y, Maruyama T, Azuma T, Miyashita Y, Mori H, Imanishi K, Takeda N, Ochi T, Otsubo M, Asahina D, Miyakawa A (2016) Characteristics of the surface ruptures associated with the 2016 Kumamoto earthquake sequence, Kyushu, southwestern Japan. In: Paper presented at the Japan Geoscience Union meeting, Chiba, Japan, 22–26 May 2016 (MIS34-P45)
- Tobita M (2003) Development of SAR interferometry analysis and its application to crustal deformation study. *J Geod Soc Jpn* 49:1–23 (in Japanese with English abstract)
- Tobita M, Fujiwara S, Murakami M, Nakagawa H, Rosen PA (1999) Accurate offset estimation between two SLC images for SAR interferometry. *J Geod Soc Jpn* 45:297–314 (in Japanese with English abstract)
- Toda S, Kaneda H, Okada S, Ishimura D (2016) Slip-partitioned surface ruptures for the M_w 7.0 2016 Kumamoto, Japan, earthquake. In: Paper presented at the Japan Geoscience Union meeting, Chiba, Japan, 22–26 May 2016 (MIS34-P48)
- Watanabe K (1978) Studies on the Aso pyroclastic flow deposits in the region to the west of Aso caldera, southwest Japan, I: geology of the Aso-4 pyroclastic flow deposits. *Mem Fac Educ Kumamoto Univ* 27:97–120
- Wei M, Sandwell D, Fialko Y, Bilham R (2011) Slip on faults in the Imperial Valley triggered by the 4 April 2010 M_w 7.2 El Mayor-Cucapah earthquake revealed by InSAR. *Geophys Res Lett.* doi:10.1029/2010GL045235
- Yarai H, Kobayashi T, Morishita Y, Fujiwara S, Munekane H, Hiyama Y, Kawamoto S, Miyahara B, SAR Analysis Group, GEONET Analysis Group (2016) Crustal deformation of the 2016 Kumamoto Earthquake. In: Paper presented at the Japan Geoscience Union meeting, Chiba, Japan, 22–26 May 2016 (MIS34-03)

Submit your manuscript to a SpringerOpen® journal and benefit from:

- Convenient online submission
- Rigorous peer review
- Immediate publication on acceptance
- Open access: articles freely available online
- High visibility within the field
- Retaining the copyright to your article

Submit your next manuscript at ► springeropen.com